Polymeric Hybrid Coatings on Ti50%Zr Alloy

MARIA VARDAKI, DANIELA COVACIU ROMONTI, DANIELA IONITA, IOANA DEMETRESCU*
University Politehnica of Bucharest, Faculty of Applied Chemistry and Materials Science, 1-7 Polizu, 011061, Bucharest, Romania

The aim of this study was to point out the effect of elaboration parameters on the structure and electrochemical stability of a bioinspired hybrid film chitosan with hydroxiapatite (HAp) on Ti50%Zr alloy. The new hybrid films based on chitosan and hydroxiapatite were elaborated electrochemically using various ratio between components and different temperature and time of electrodeposition. The electrodeposition electrolye was a mixture of $(NH_4)_2HPO_4$, $Ca(NO_3)_2$ and chitosan. The structure was identified by Fourier transform infrared (FTIR) spectroscopy, and the morphology associated with elemental analysis were evaluated by scanning electronic microscopy (SEM) and X ray diffraction. Surface characterization was completed with contact angle measurements. Electrochemical tests in physiological solution (NaCl 0.9%) potentiodinamic polarization curves (tafel plots procedures). Based on experimental data we can conclude that the hybrid coating with higher HAp concentration is the most stable.

Keywords: chitosan, hydroxyapatite, TiZr, electrodeposition, FTIR, SEM, electrochemical stability

Enhancing biomaterials performance building nanostructure as nanotubes [1] and nanochaneles [2] or coating with various materials are widely used procedures in metallic surface modifications in the last decades. For coatings, hybrid materials represent a good choice taking into account that each material in such a combination is going to introduce specific complementary properties according to a previous design [3]. There are a large number of bioinspired polymeric coating based on natural polymeric material as collagen and chitosan [4,5]. In the nomenclature proposed by the European Chitin Society (EUCHIS) chitin and chitosan should be classified on the basis of their solubility and insolubity in 0.1 M acetic acid, the soluble material being chitosan [6]. Chitosan is a smart natural polymer based on the fact that its solubility is changing in response to a stimulus as *p*H [7].Chitosan is a termoresponsive polymer as well. Nowadays, smart polymers as chitosan responding to various stimuli has extended their applications are intensively recommended for the controlled delivery of drugs [8]. In the same time chitosan is one of the few materials presenting, bioactivity, biodegradability and osteoconductivity [9]. Designing a composite material based on combination of both biodegradable, bioactive and osteoconductive components, meaning natural polysaccharide chitosan and ceramic HAp should be a positive approach in elaboration of suitable materials for scaffold fabrication [10]. Coatings with such hybrid materials on metallic alloys for tissue engineering it will be a guarantee of enhanced tailored physical, biological and mechanical properties as well as predictable degradation. It is to mention that Ti and Ti alloys have impressive stability and biocompatibility [11,12] and its alloying is due to improve mechanical properties. Of course for Ti aloying nontoxic and non allergenic elements as Nb and Zr are suitable choices and Ti50%Zr 50% was already recommended for its stability [13,14] and antibacterial effects [15]. To our knowledge cathodic deposits of various thicknesses and components concentrations of chitosan and HAp were obtained on a large number of substrates [16,17] as Pt, stainless steel foils, and graphite, but Ti50%Zr was not one of the modified substrate. However, elaboration of a hybrid coating based on chitosan on Ti50% Zr surface and the electrochemical stability characterization of coatings has not been investigated until now. It is the aim and the novelty of this manuscript to study the effect of two concentrations of HAp on the structure and electrochemical stability of bioinspired electrodeposited hybrid coating chitosan and HAp.

Experimental part

Materials and methods

Samples preparation

As a substrate, Ti50%Zr samples were used. The samples were cleaned by wet grinding using SiC paper 800, 1200 and 2400 grit. After polishing the samples were cleaned in an ultrasound bath with ethanol for 5 minutes, rinsed with distilled water and dried at room temperature.

Preparation of electrolyte solutions and deposition of the hybrid coating

For electrodeposition, the used the electrolyte was a mixture between $Ca(NO_3)_2 \cdot 4H_2O$ (0.042 M) + $NH_4H_2PO_4$ (0.025 M) and chitosan (0.5g/ L in acetic acid). The chemicals were provided by Sigma Aldrich. The deposition of the hybrid coating was performed with different parameters, as it is presented in table 1. The electro-deposition process was carried out using amperometric techniques with a potential of -1.3 V and 60 min for deposition.

In order to optimize the best deposition parameters some series of coated samples were performed under various conditions as it is presented in table 1.

The coated TiZr samples with hydroxyapatite (HAp) and chitosan (CS) were thermally treated for strengthening the bonds of apatite coatings and to increase the crystallinity and the purity of the coating.

Selected coated samples were HAp:CS = 1:1 and HAp:CS = 2:1, deposited at 37°C, and dried at 37°C. These samples presented the most uniform coating and the best adhesion with the metallic surface.

Characterization of polymeric hybrid coatings

Surface morphology was carried out by scanning electron microscopy (SEM, Hitachi S-4160). The coating characterization was carried out with an D8 DISCOVER

* email: ioana_demetrescu@yahoo.com

HA/CS Proportion	Deposition time [min]	Deposition temperature [°C]	Thermal treatment/ time [°C]
1:1	60	80/ 37	400
2:1	60	80/ 37	400
1:1	60	80/ 37	37
2:1	60	80/ 37	37

Table 1
ELECTRODEPOSITION CONDITIONS FOR TiZr SAMPLES

(Bruker Axs) Difractometer, by using as X-ray source a cathode from Cu(Kα=1.54060Å), mirror Gõbell - 0.6 mm and Lynx-Eye detector 1D, according to SR EN 13925:2003: Non-destructive testing. X-ray diffraction from poly-crystalline and amorphous materials.

The FT-IR spectroscopic analysis on coated TiZr samples for phosphate masses and chitosan detection was carried out with Perkin Elmer FTIR spectrophotometer (Spectrum 100 Model) with an attenuated total reflection accessory ATR.

The contact angle measurements of a drop of distilled water with the coating surface were done with a CAM 100 Equipment. All the measurements were performed with distilled water. The obtained values represent the average from 5 determinations.

Electrochemical measurements

Electrochemical measurements were carried out using a Voltalab Potentiostat/ Galvanostat PGZ 301 equiped with Volta Master Sofware. The system used for electrochemical determinations was a three electrode cell with a reference electrode Ag/AgCl (3M), working electrode as TiZr samples and Pt as a counterelectrode. The exposed area, to electrolyte solution of the samples was 1 cm^2. The electrolyte solution for electrochemical tests was physiological serum with a content of 0.9% NaCl in distilled water, prepared at room temperature. Electrochemical tests include measurements of potentiodinamic polarization curves. Electrochemical parameters as polarization resistance (R_p), corrosion current (i_{corr}) or corrosion rate (v_{corr}), anodic and cathodic constants (B_a, B_c) were determined from Tafel curves using [-200 ÷ 200 mV] for start and stop potential and a scan rate of 0.0001 V/s. The experimental data were processed using Origin Software, version 11.

Results and discussions

Surface characterization and morphology

Figure 1 shows the SEM images of hydroxyapatite/ chitosan composites. All the SEM images of composites are considered highly porous structure. The size of the pores was fluctuating around 100-250 μm and the HAp particles were embedded well in the chitosan matrix.

The increase of hydroxyapatite content results in the decrease of pores size, whereas the thickness of the cavities between cells was reduced.

As can be seen in figure 2, when the amount of the chitosan was decreased and the quantity of hydroxyapatite was increased, the density of the composite was also increased which led to the decrease of porosity.

For a pure HAp sample, the existence of 2θ peaks at approximately 26.0°, 31.4°, 32.2° and 40.1° was recorded, corresponding to the diffraction planes (002), (211), (300), (310) respectively (JCPDS: 86-0749). The pattern confirms the presence of crystalline HAp obtained via the applied

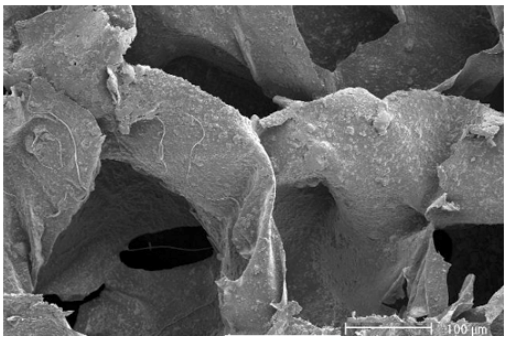

Fig. 1. SEM images of TiZr coated with HAp:CS = 1:1

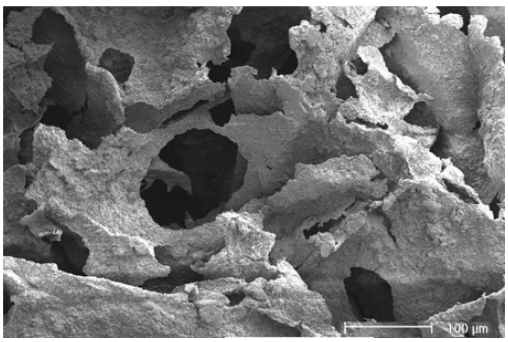

Fig. 2. SEM images of TiZr coated with HAp:CS = 2:1

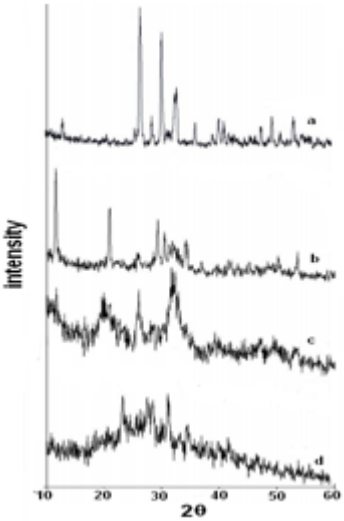

Fig. 3. X-ray diffraction of synthesized composites with different amount of HAp ratio (a) HAp; b) HAp:CS = 2:1; c) HAp:CS = 1:1, d) CS

method. Characteristic interferences for pure chitosan were located around 25° [18]. The obtained composite with a lower amount of hydroxiapatite shows a visible broadening of the mineral diffraction peaks, suggesting a diminishing size of the apatite crystals and a decrease in its crystallinity [19, 20]. Broadening and weakening of the characteristic inteferences of the mineral as well as of the polymer matrix after the formation of the composite indicate the bonding of the two phases.

The FT-IR spectra of pure CS and HAp and of composites with various HAp/CS ratios are shown in figure 4.

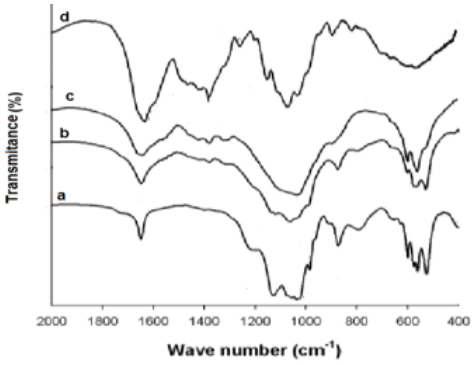

Fig. 4. FT-IR analysis of: a) HAp ; b) HAp:CS = 2:1; c) HAp:CS = 2:1, d) CS

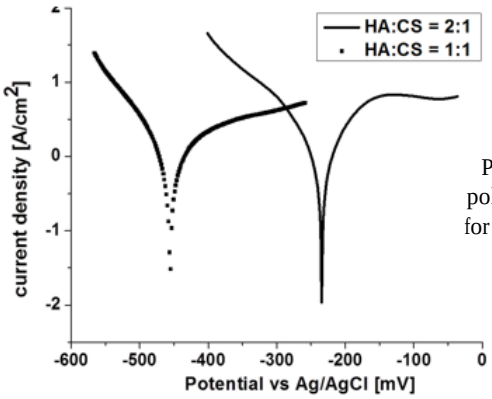

Fig. 5. Potentiodinamic polarization curves for HA:CS = 2:1 and HA:CS = 1:1

Coated TiZr	R_p [KΩcm^2]	I_{corr} [μA]	B_a [mV]	B_c [mV]	v_{corr} [μm/year]
HA:CS = 1:1	18.56	1.05	221	-83	20.45
HA:CS = 2:1	132.77	0.234	220	-116	4.55

Table 2
CORROSION PARAMETERS FOR COATED TiZr SAMPLES

The characteristic spectrum of HAp is mainly found at lower wave numbers. Phosphate bands can be seen at 474, 572, 601, 972, 1040 and 1100 cm^{-1} [21]. The phosphate bands at 572 and 601 cm^{-1} were due to a phosphate bending and the absorption bands at 972, 1040 and 1100 cm^{-1} were indicative of a phosphate stretching [22]. The absorption bands at 633 and 3570 cm^{-1} represented OH vibration. The band at 1660 cm^{-1} represented the water absorption. Carbonate bands were observed at 870 cm^{-1} and 1430 cm^{-1} [23]. The FT-IR spectrum of pure CS shows a characteristic bands around 1650 cm^{-1} and 1600cm $^{-1}$ indicating the =C=O stretching vibrations and the =N–H in-plane bending vibrations characteristic of amide I and II structures. Also a band characteristic of the amide III structure is visible at 1257 cm^{-1}, whose intensity decreases with the increase of HAp content in the composite. Band around 2925 cm^{-1} was attributed to –CH backbone vibrations, while a band around 1400 cm^{-1} was attributed to $-CH_3$ and $-CH_2$ in-plane deformation. A series of absorption bands around 1070 cm^{-1} most likely corresponds to glucosamine stretching vibrations.

The FTIR spectrum of the composites with various HAp/CS ratios reveals some important changes. The band related to the –CH backbone vibrations of CS clearly decreases in intensity as HAp content increases. Strong deformations of the β-1,4-glycosidic linkage throughout the composite set up, were represented by the peak with maximum at 896 cm^{-1}, are confirmations of hydrogen interactions between HAp and CS. The disappearance/deformation of the ether bond in the pyranose ring at 1153 cm^{-1} and the amide III band at 1257 cm^{-1} serves as additional evidence for the chemical interconnection of the two phases.

In order to establish hydrophobic-hydrophilic balance, contact angle measurements were performed on coated and uncoated samples of TiZr. The smallest value of the contact angle was determined for HA:CS = 1:1 (19°) compared with uncoated TiZr (70°), denoting a high porosity and a high hydrophilicitity. For HA:CS = 2:1 sample, the recorded value for contact angle was 40°, which confirm the existence of a more dense structure with small pores of the coating. All the obtained data from contact angle measurements are in accordance with the morphology characterization.

Electrochemical measurements

Corrosion parameters were determined from polariozation curves, using Tafel procedures. The coated samples of TiZr were tested in physiological serum (NaCl 0.9%). In figure 5. are presented potentiodinamic polarization curves for HA:CS = 2:1 and HA:CS = 1:1.

According to the obtained polarization curves it can be noticed the fact that the best behaviour of the coated samples in NaCl 0.9% solution is for the sample coated with the highest amount of hydroxyapatite. The HA:CS = 2:1 sample present the smallest corrosion current comparing with the sample HA:CS = 1:1. The obtained value of the polarization resistance increase with the increasing oh the hydroxyapatite amount. In Table 2 it can be observed that R_p is approximately 8 times higher for HA:CS = 2:1 than for HA:CS = 1:1.

Also from table 2 it can be noticed that the smallest corrosion rate was obtained for the TiZr sample coated with the highest concentration on hydroxyapatite. All the obtained data from electrochemical data and corrosion behavior are in accordance with the morphology and surface characterization.

Conclusions

A range of various conditions of elaboration of a bioinspired hybrid coating based on chitosan and hydroxyapatite have been proposed and tested on Ti50%Zr alloy. The conditions include time of stirring and time or temperature of electrodeposition. Based on experimental data as FTIR, SEM, XRD and contact angle determinations, structure, morphology and the balance hydrophilic hydrophobic of the surface coatings have been evaluated. Electrochemical tests in physiological solutions identified the coating with higher concentration of HAp obtained at the human temperature as the most stable coating.

Acknowledgements: The work has been funded by the Sectoral Operational Programme Human Resources Development 2007-2013 of the Ministry of European Funds through the Financial Agreement POSDRU/159/1.5/S/134398.

References

1. MAN, I., PIRVU, C., DEMETRESCU, I., Rev. Chim. (Bucharest), **59**, no. 6, 2008, p. 615.
2. MANOLE, C.C., PIRVU, C., STOIAN, A.B., CALDERON MORENO, J.M., STANCIU, D., DEMETRESCU, I., J. Nanomat., 2015, Article ID 521276, 9 pages.
3. GAREA, S.A., MIHAI, A.I., GHEBAUR, A., Mat. Plast., **52**, no. 3, 2015, p. 275.

4. BONDERER, L.J., STUDART, A.R., GAUCKLER, L.J., Science, **319**, no. 5866, 2008, p. 1069.
5. NEDELCU, I.-A., FICAI, A., FICAI, D., VOICU, G., ALBU, M.G., ANDRONESCU, E., UPB Sci. Bull., Series B: Chemistry and Materials Science, 77, no. 1, 2015, p. 3.
6. ROBERTS, G.A.F., Adv. Chitin. Sci., 10, 2007, p.3.
7. WARD, M.A., GEORGIOU, T.K., Polymers, **3**, 2011, p. 1215.
8. JAMES, H.P., JOHN, R. ALEX, A., ANOOP, K.R., Acta Pharm. Sinica B, **4**, nr. 2, 2014, p. 120.
9. KONG, L., GAO, Y., LU, G., GONG, Y., ZHAO, N., ZHANG, X., Eur. Polym. J., **42**, 2006, p. 3171
10. LIU, Z., HAN, J., CZERNUSZKA, T., Acta Biomat., **5**, 2009, p. 661.
11. MINDROIU, M., CICEK, E., MICULESCU, F., DEMETRESCU, I., Rev. Chim. (Bucharest), **58**, no. 9, 2007, p. 898
12. IONITA, D., GRECU, M., UNGUREANU, C., DEMETRESCU, I., App. Surf.Sci., **21**, 2011, p. 9164.
13. KIM, W.G., CHOE, H.C., KO, Y.M., BRANTLEY, W.A., Electrochemical characteristics of nanotube formed Ti-Zr alloy, NSTI-Nanotech, **1**, 2008, p. 462.
14. KIM, W.G., CHOE, H.C., Trans. Nonferrous Met. Soc. China, 19, 2009, p. 1005.
15. GRIGORESCU, S., UNGUREANU, C., KIRCHGEORG, R., SCHMUKI, P., DEMETRESCU, I., App. Surf. Sci., 270, 2013, pp. 190.
16. PANG, X., ZHITOMIRSCHI, I., Mater. Chem. Phys., **94**, no. 2–3, 2005, p. 245.
17. PANG, X., CASAGRANDE, T., ZHITOMIRSKY, I., J. Colloid Interface Sci., **330**, 2009, p. 323.
18. ZHANG, Y., ZHANG, M., J. Non-Cryst. Solids., **282**, 2001, p. 159.
19. LI, X.Y., NAN, K.H., SHI, S., CHEN, H., 2012, Int. J. Biol. Macromol., **50**, p. 43.
20. NIKPOUR, M.R., RABIEE, S.M., JAHANSHAHI, M., Compos.: Part B, **43**, 2012, p. 1881.
21. YUXIU, S., GUANGSHENG, G., ZHIHUA, W., HONGYOU, G., Ceram. Int., **32**, no. 8, 2006, p. 951.
22. CHEN, F., WANG, Z.C., Lin, C.J., Mater. Lett., 57, 2002, p. 858.23. YAMAGUCHI, I., TOKUCHI, K., FUKUZAKI, H., KOYAMA, Y., TAKAKUDA, K., MONMA, J.TANAKA, H., J. Biomed. Mater. Res., 55, 2001, p. 20.
23. YAMAGUCHI, I., TOKUCHI, K., FUKUZAKI, H., KOYAMA, Y., TAKAKUDA, K., MONMA, J.TANAKA, H., J. Biomed. Mater. Res., 55, 2001, p. 20

Manuscript received: 6.11.2015